Supplementary materials

Hydrodynamic selection determines whether retained biomass undergoes mechanical maturation or aggregate enlargement during continuous-flow anammox granulation

Text S1 EPS

Seed sludge and granular sludge collected on days 92 and 121 were selected to determine EPS contents and to further analyze stage-dependent changes in sludge characteristics. EPS were extracted using a heating extraction method, yielding three EPS fractions: soluble EPS (S-EPS), loosely bound EPS (LB-EPS), and tightly bound EPS (TB-EPS). The protein (PN) and polysaccharide (PS) contents of the extracted EPS were quantified according to the method described by Zhu et al.(2023).

The sludge was further characterized using three-dimensional fluorescence spectroscopy (F-4700, Hitachi, Japan). The excitation wavelength was scanned from 200 to 800 nm with 10 nm intervals, while the emission wavelength ranged from 200 to 800 nm with 1 nm intervals; the slit width was set to 10 nm. In addition, parallel factor (PARAFAC) analysis was conducted using the DOMFluor toolbox implemented in MATLAB R2024a (MathWorks Inc., USA). The DOMFluor toolbox was applied to decompose excitation–emission matrix (EEM) data and identify variations in EPS components.

Text S2 Rheological properties

To compare the physical properties of anammox granular sludge under different shear forces, the storage modulus (G'), loss modulus (G"), and complex viscosity (η*),

which reflect the mechanical strength and rheological behavior of the biomass, were determined following the method described by Lin and Wang(2017).

Text S3 Surface thermodynamics

The zeta potentials and contact angles of R1 and R2 with water, formamide, and 1-bromonaphthalene were measured for seed sludge and sludge collected on days 92 and 121 using a zeta potential analyzer (Zetasizer Nano ZS90, Malvern, UK) and a contact angle analyzer (OCA20, DataPhysics, Germany), respectively. Surface thermodynamic analysis was conducted based on the measured contact angles and ζ potentials to evaluate particle aggregation and growth tendencies. According to the theoretical framework described by Wang et al.(2021), the microbial total interaction energy (W_{TOT}), van der Waals interaction energy (W_A), acid–base interaction energy (W_{AB}), and electrostatic interaction energy (W_R) were calculated.

Text S4 Extended DLVO theory

In the extended DLVO theory, the Lewis acid-base hydration force (W_{AB}) is included and the total energy of the microbial cell interaction (W_{TOT}) is expressed as the sum of the electrostatic repulsion of the electric double-layer interaction (W_R), the van der Waals energy (W_A), and (W_{AB}): $W_{TOT}=W_R+W_A+W_{AB}$ (Grasso et al., 2002a). All of the interaction energies are related to the separation distance H, and are used to analyze the distance-dependent interrelationship of different interaction energies. The calculation of surface thermodynamics and extended DLVO theory was according to the formulas described by (Hou et al., 2015). The total surface tension (γ) is the sum of apolar van der Waals surface tension component γ^{LW} and apolar or acid-based

surface tension component γ^{AB}. $\gamma^{AB}=2\sqrt{\gamma^{+}\gamma^{-}}$, so the total surface tension of bacteria (γ_B) and liquid (γ_L) can be expressed as following:

$$\gamma_B=\gamma_B^{LW}+\gamma_B^{AB}=\gamma_B^{LW}+2\sqrt{\gamma_B^{+}\gamma_B^{-}} \quad (S1)$$

$$\gamma_L=\gamma_L^{LW}+\gamma_L^{AB}=\gamma_L^{LW}+2\sqrt{\gamma_L^{+}\gamma_L^{-}} \quad (S2)$$

The surface tension component and parameters of bacteria were calculated with the following equation.

$$(\gamma_L^{LW}+2\sqrt{\gamma_L^{+}\gamma_L^{-}})\ (1+\cos\theta)=2(\sqrt{\gamma_S^{LW}\gamma_L^{LW}}+\sqrt{\gamma_S^{+}\gamma_L^{-}}+\sqrt{\gamma_S^{-}\gamma_L^{+}}) \quad (S3)$$

Where θ is the contact angle of the bacteria by the drop of the liquid to the surface of the microorganism; γ_L^{+},γ_L^{-} are electron-acceptor andelectron-donor parameters in the Lewis acid-base water hydration for water; γ_B^{+},γ_B^{-} are electron-acceptor andelectron-donor parameters in the Lewis acid-base water hydration for testing microbial cells.

Therefore, Van der Waals surface tension and Polar force between microorganisms and water can be expressed as following:

$$\gamma_{BL}^{LW}=(\sqrt{\gamma_B^{LW}}-\sqrt{\gamma_B^{LW}})^{2} \quad (S4)$$

$$\gamma_{BL}^{AB}=2(\sqrt{\gamma_B^{+}\gamma_B^{-}}+\sqrt{\gamma_L^{+}\gamma_L^{-}}-\sqrt{\gamma_B^{+}\gamma_L^{-}}-\sqrt{\gamma_L^{+}\gamma_B^{-}}) \quad (S5)$$

The different interfacial free energy between the microorganisms and water could be expressed as following (Gueto-Tettay et al., 2011):

$$\Delta G_{adh}^{LW}=-2\gamma_{BL}^{LW} \quad (S6)$$

$$\Delta G_{adh}^{AB}=-2\gamma_{BL}^{AB} \quad (S7)$$

$$\Delta G_{adh}=\Delta G_{adh}^{LW}+\Delta G_{adh}^{AB}=-2\ (\gamma_{BL}^{LW}+\gamma_{BL}^{AB}) \quad (S8)$$

The DLVO theory is used to describe the interaction between flocs in an

activated sludge-water system.

$$W_A = -\frac{A_{BLB} R}{12H} \quad \text{(S9)}$$

$$W_R = 2\pi\varepsilon R\psi^2 \ln(1+\exp(-\kappa H)) \quad \text{(S10)}$$

$$W_{AB} = \pi R\lambda G_{adh}^{AB} \exp(\frac{l_0 - H}{\lambda}) \quad \text{(S11)}$$

Where, A_{BLB} is the effective Hamaker constant, R is microbial radius; H is separation distance between the bacterias; l_0 is minimum equilibrium distance between the two surfaces (≈0.157 nm); ε is a dielectric constant; Ψ and k are the Stern potential and the thickness of the diffusion electric double layer, respectively, and Ψ can be replaced by Zeta potential at low concentrations; λ is the correlation length of the hydracy layer in the water for microbial cells (Grasso et al., 2002b).

Effective Hamaker constant can be expressed as following (Liu et al., 2008):

$$A_{BLB} = (\sqrt{A_{BB}} - \sqrt{A_{LL}})^2 = 24\pi l_0^2 (\sqrt{\gamma_B^{LW}} - \sqrt{\gamma_L^{LW}})^2 \quad \text{(S12)}$$

References:

Grasso, D., Subramaniam, K., Butkus, M., Strevett, K., Bergendahl, J., 2002a. A review of non-DLVO interactions in environmental colloidal systems. Reviews in Environmental Science and Biotechnology 1, 17-38.

Hou, X., Liu, S., Zhang, Z., 2015. Role of extracellular polymeric substance in determining the high aggregation ability of anammox sludge. Water Res. 75, 51-62.

Gueto-Tettay, C., Drosos, J.C., Vivas-Reyes, R., 2011. Quantum mechanics study of the hydroxyethylamines-BACE-1 active site interaction energies. J. Comput. Aided. Mol. Des. 25, 583-597.

Grasso, D., Subramaniam, K., Butkus, M., Strevett, K., Bergendahl, J., 2002b. A review of non-DLVO interactions in environmental colloidal systems. Reviews in Environmental Science and Biotechnology 1, 17-38.

Lin, X. and Wang, Y. 2017. Microstructure of anammox granules and mechanisms endowing their intensity revealed by microscopic inspection and rheometry. Water Research 120, 22-31.

Liu, X.M., Sheng, G.P., Wang, J., Yu, H.Q., 2008. Quantifying the surface characteristics and flocculability of Ralstonia eutropha. Appl. Microbiol. Biotechnol. 79, 187-194. https://doi.org/10.1007/s00253-008-1426-1

Zhu, Y., Chen, G., Yu, D., Liu, R., Chen, X., Yang, Z., Yao, T., Gong, Y., Shan, Y. and Wang, Y. 2023. Sludge composting with self-produced carbon source by phosphate buffer coupled hyperthermophilic pretreatment realizing nitrogen retention. Chemical Engineering Journal 476, 146811.

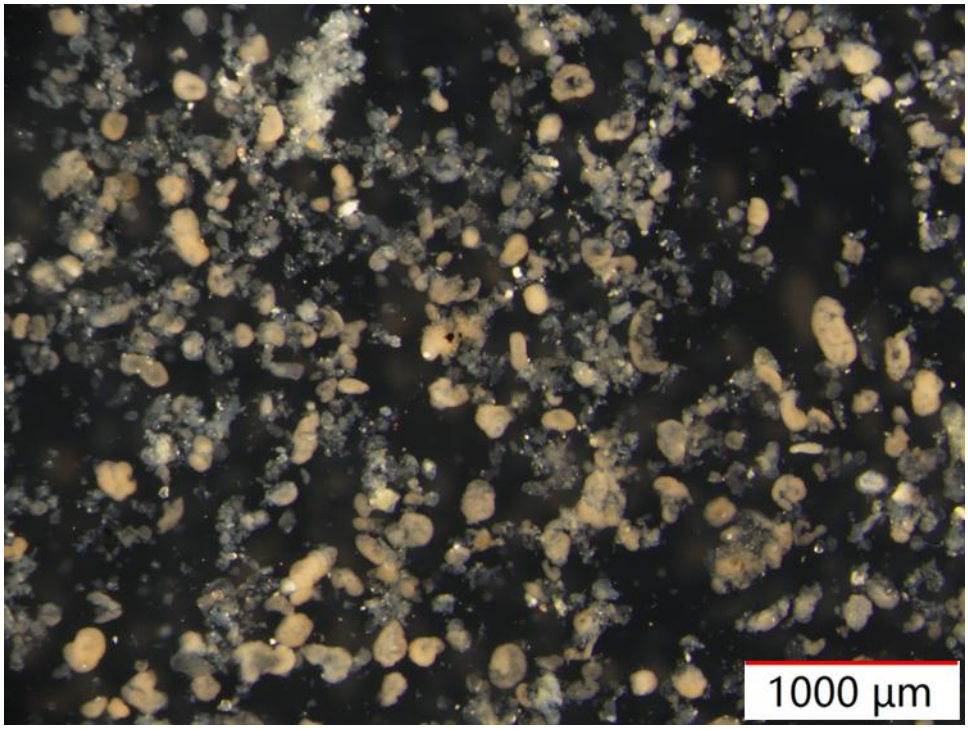


Fig. S1 Microscopic image of the seed sludge before reactor inoculation.

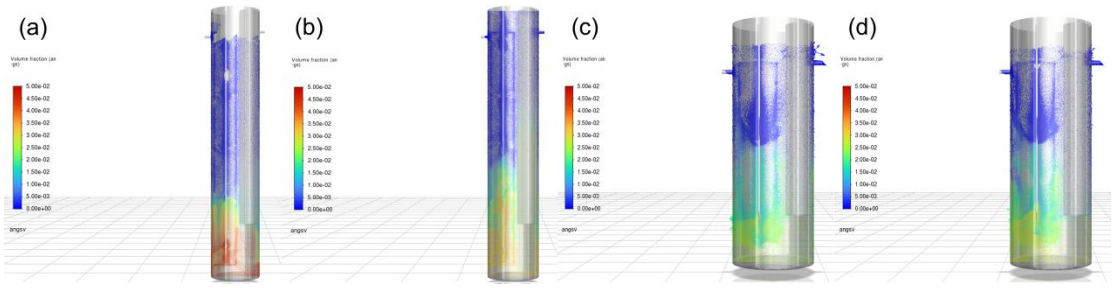


Fig. S2 CFD-simulated sludge distribution, and velocity vectors in reactors with different height-to-diameter ratios. (a, b) Sludge volume fraction and velocity vectors in R1 at 150 and 180 r/min. (c, d) Sludge volume fraction and velocity vectors in R2 at 150 and 120 r/min.

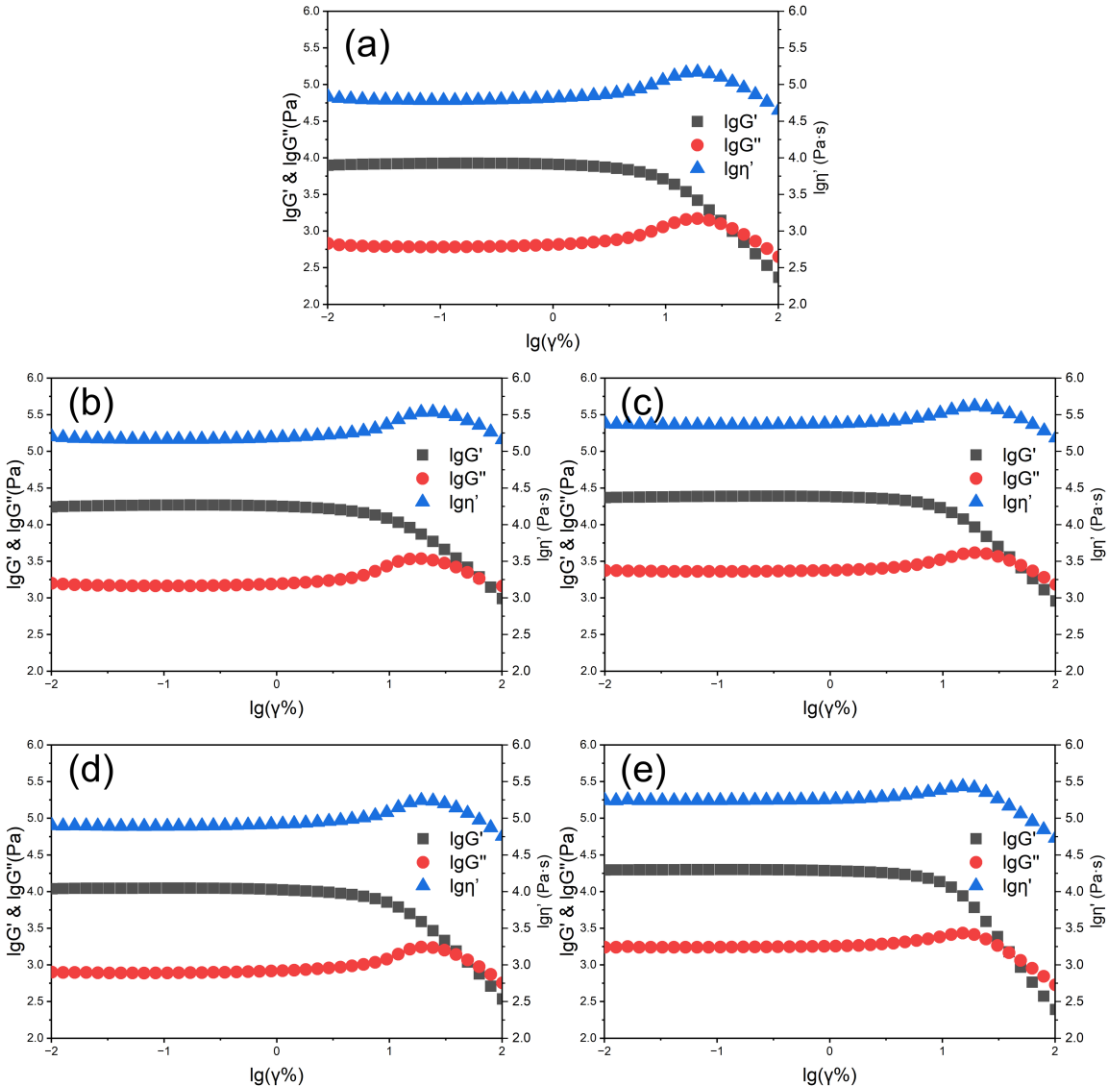


Fig. S3 Rheological properties of anammox sludge at different stages. (a) Seed, (b) R1-92, (c) R1-121, (d) R2-92, and (e) R2-121. Storage modulus (G′), loss modulus (G″), and complex viscosity (η*) are shown.

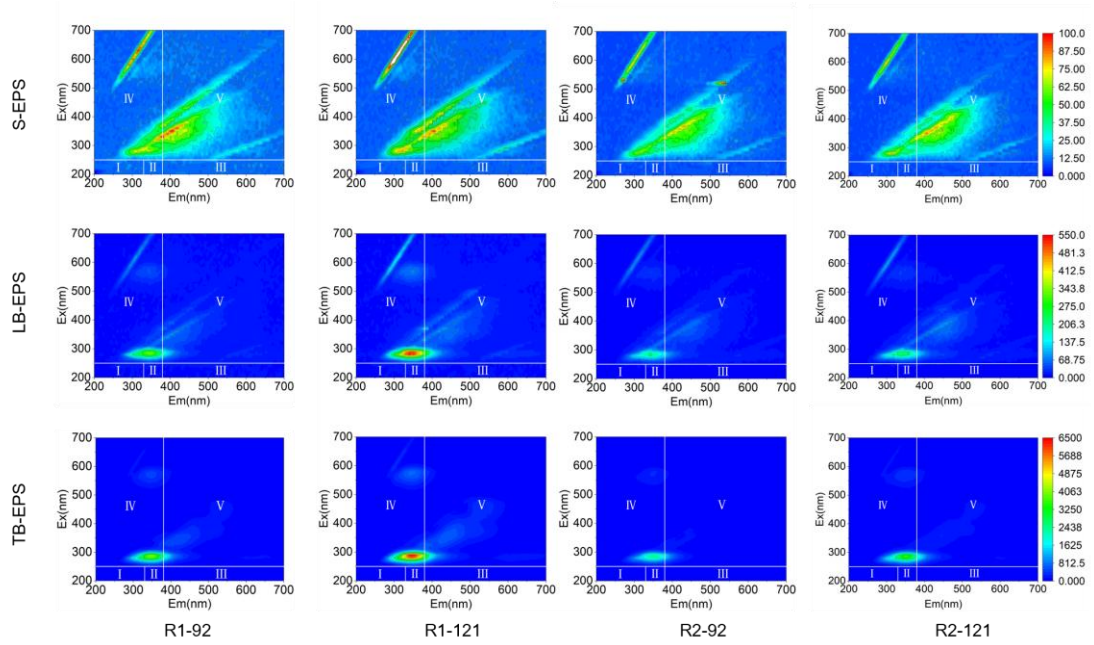


Fig. S4 Three-dimensional fluorescence spectra of particles at different stages.

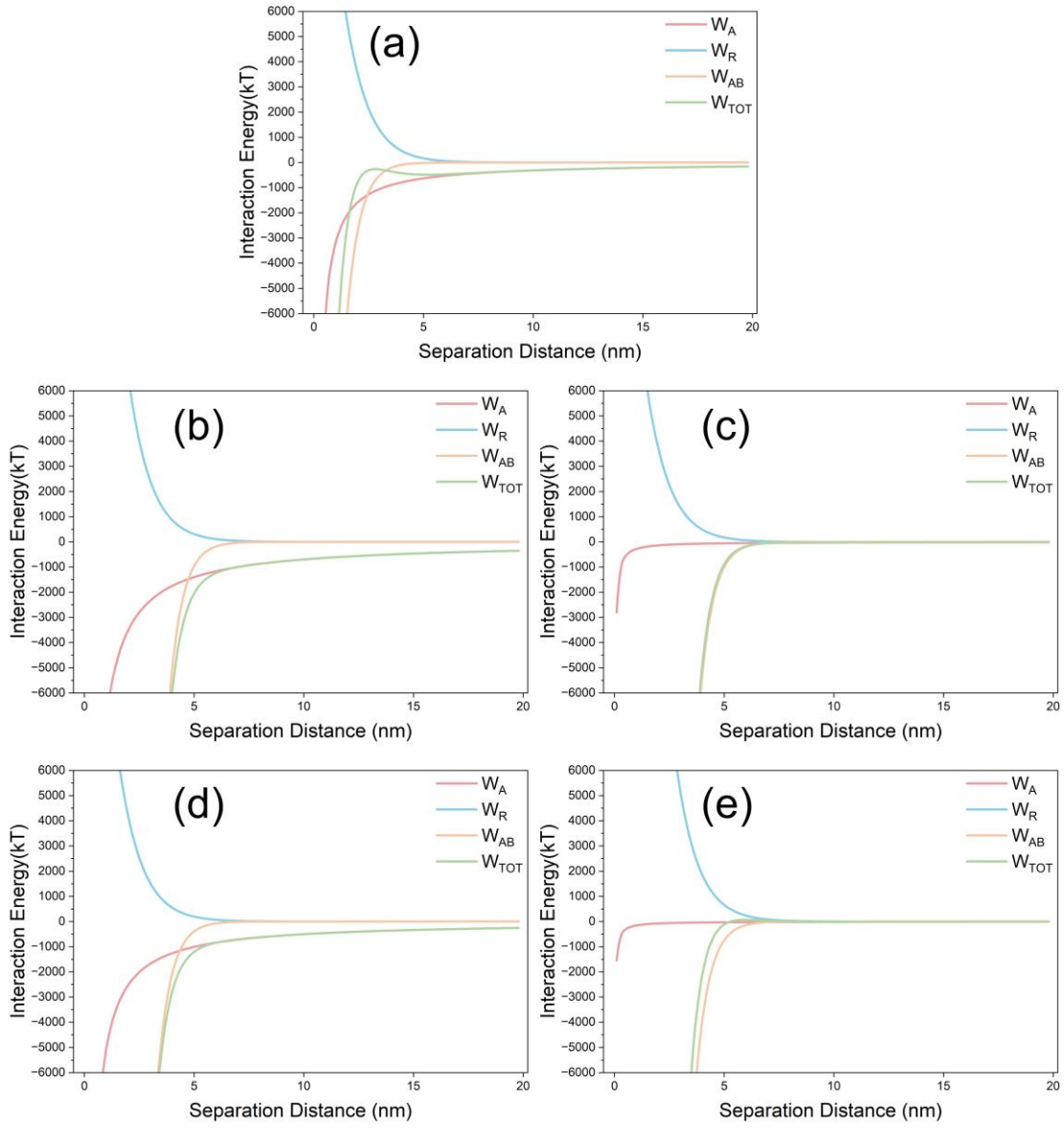


Fig. S5 XDLVO total interaction-energy profiles of sludge samples at different stages.

(a) Seed, (b) R1-92, (c) R1-121, (d) R2-92, and (e) R2-121.

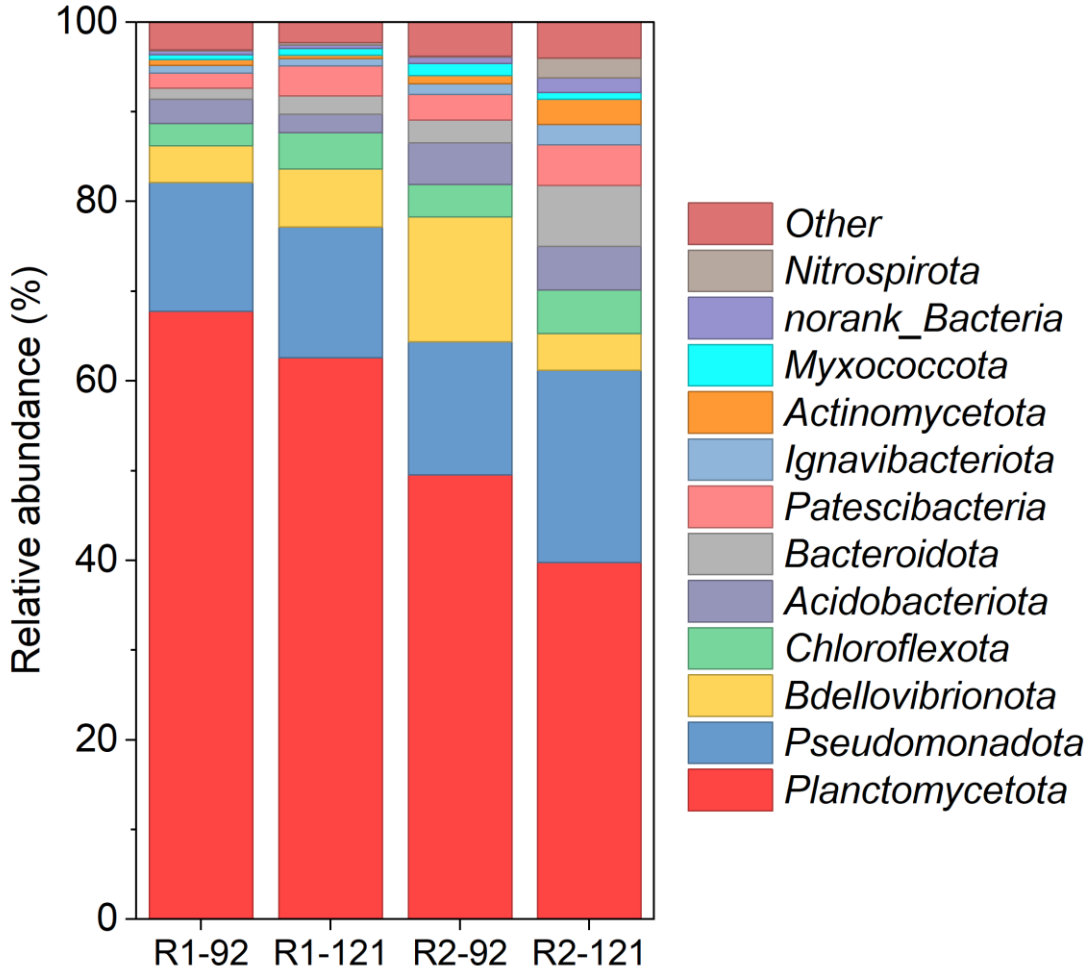


Fig. S6 Phylum-level microbial community composition of R1 and R2 on days 92 and 121.

Table S1 Granule size of anammox

Sample	D10 (μm)	D50 (μm)	D90 (μm)	D[4,3] (μm)
Seed	24.09	65.75	143.90	90.11
R1-46	66.9	168.54	351.67	227.58
R1-92	111.47	269.78	515.77	344.72
R1-121	163.49	343.51	586.00	412.34
R2-46	66.9	178.97	309.53	202.96
R2-92	185.75	300.61	665.79	339.80
R2-121	272.43	392.94	589.45	537.59

Table S2 Hydrodynamic parameters and corresponding granule characteristics under different operating conditions

Reactor condition	P/V (W/m^3)	Volume-averaged ε (m^2/s^3)	Area-weighted mean WSS (Pa)	D[4,3] (μm)	G′ (kPa)	SCI (Pa/μm)
R1–150 r/min (day 92)	56.8	0.0152	0.212	344.72	19.74	57.26
R1–180 r/min (day 121)	107.4	0.0255	0.343	412.34	23.43	56.82
R2–150 r/min (day 92)	27.7	0.00549	0.127	339.80	17.49	51.47
R2–120 r/min (day 121)	14.8	0.00318	0.0867	537.59	10.93	20.34

Note: P/V, stirring power density; ε, volume-averaged turbulent dissipation rate; WSS, area-weighted mean wall shear stress; SCI, structural compactness index.

Table S3 Surface adhesion free-energy components of different sludge samples

Sludge	ΔG_{adh}^{LW} **(mJ/m^2)**	ΔG_{adh}^{AB} **(mJ/m^2)**	ΔG_{adh} **(mJ/m^2)**
Seed	-3.744	-2.836	-6.58
R1-92	-2.158	-38.772	-40.93
R1-121	-0.072	-34.032	-34.10
R2-92	-1.574	-16.132	-17.71
R2-121	-0.031	-19.340	-19.37